Solar-terrestrial conditions during SUNDIAL-86 and empirical modelling of the global-scale ionospheric response

E.P. SZUSZCZEWICZ (¹), P. WILKINSON (²), M.A. ABDU (³), E. ROELOF (⁴),
R. HANBABA (⁵), M. SANDS (¹), T. KIKUCHI (⁶), R. BURNSIDE (⁷),
J. JOSELYN (⁸), M. LESTER (⁹), R. LEITINGER (¹⁰), G.O. WALKER (¹¹),
B.M. REDDY (¹²), and J. SOBRAL (³)

(¹) *Laboratory for Atmospheric and Space Sciences, Science Applications International Corporation, McLean, Virginia 22102. U.S.A.*
(²) *IPS, Australia.*
(³) *INPE, Brazil.*
(⁴) *Johns Hopkins Applied Physics Laboratory, U.S.A.*
(⁵) *CNET, France.*
(⁶) *Ministry of Post and Telecommunications, Japan.*
(⁷) *Arecibo Observatory, Puerto Rico.*
(⁸) *NOAA, U.S.A.*
(⁹) *University of Leicester, U.K.*
(¹⁰) *University of Graz, Austria.*
(¹¹) *University of Hong Kong, H.K.*
(¹²) *National Physical Laboratory, India.*

ABSTRACT. Covering the period from 22 September through 4 October 1986, the SUNDIAL-86 Solar-Minimum Equinoctial Campaign studied the behavior of the global-scale ionosphere. The period covered the most quiet (Q1) and second most disturbed (D2) days of the entire month of September, with the disturbed conditions triggered by a high-speed solar wind stream. Ionospheric responses were monitored by the SUNDIAL network of nearly 70 stations distributed approximately in three longitudinal domains; and global maps of f_oF_2 results were compared with the « predictions » of the International Reference Ionosphere modified to include an empirical specification of auroral oval boundaries and associated high-latitude morphological domains. Comparisons that included regions in the polar cap, diffuse auroral oval, mid-latitude trough, equatorial anomaly and the sunrise/sunset terminator showed good agreement between the hourly 8-day-averaged ionospheric observations and the model. The inclusion of an auroral oval and the good agreement between model contours of f_oF_2 and SUNDIAL observations adds to the quality and applicability of the IRI and builds a foundation for the development of an adaptive time-dependent empirical model to describe global-scale ionospheric responses to storm dynamics.

1. INTRODUCTION

To understand coupling processes in the system of solar-terrestrial plasmas requires the synthesis of solar, interplanetary, magnetospheric, thermospheric and ionospheric physics. In this system, the ionosphere can be viewed as the culmination of all the contributions, and the accurate specification of ionospheric electron density distributions at any time and under any conditions can be viewed as a critical test of our understanding of the myriad of coupling terms. This is the perspective of the SUNDIAL investigation (Szuszczewicz *et al.*, 1988) with its objective being the development of a comprehensive understanding and predictive capability for handling the cause-effect relationships which govern the quiescent and disturbed states of the global-scale ionosphere. While the focus is on the ionospheric state at any place, at any time and under any condition, the program uses measurements of the solar and interplanetary inputs, and works to establish an understanding of the interactive roles that the ionosphere plays with the magnetosphere and thermosphere.

We consider ionospheric specification and prediction to involve: (1) the « quiet time » altitude profile of plasma densities at any place and time, and for any season and period within the sunspot cycle; (2) global responses of those profiles to dynamic events; and (3)

irregularity scale-size distributions under unstable geoplasma conditions. We also consider the time-frame classification of predictions as another important aspect, because it helps to qualify the type of prediction and to focus attention on the fundamental input requirements.

Current advances in solar-terrestrial physics suggest that accurate ionospheric prediction is achievable at two temporal levels. First is the intermediate term, involving periods of tens of minutes, hours, and days, with the upper limit being the 27-day solar rotation period. It is in the intermediate term that the best possibility exists for the development of genuine ionospheric prediction capabilities. The second time frame involves the longer term, periods of months and years. Here, the best that can be expected is a prediction of « average » ionospheric behavior (i.e. ionospheric climatology) for input terms characteristic of the solar and seasonal period for which the prediction is developed. Clearly, a systematically-improved intermediate-term prediction capability will enhance the quality of the predictions for the longer term.

For short-term predictions (involving ionospheric variations with time scales of the order of seconds to tens of minutes), accumulated knowledge suggests that the integrity of the predictions are faulted largely by non-deterministic processes and that the loosely scientific approach of persistence is the only prediction tool currently available. These « non-deterministic » processes can be considered to include the noise-like fluctuations of the IMF and hourly variations of f_oF_2 values about a smoothed diurnal trend. Within the SUNDIAL investigations, such features are studied for synoptic and global coherence, but as yet there have been no convincing patterns to suggest a short-term prediction capability.

The SUNDIAL series of investigations is focused on improving our understanding of solar-terrestrial coupling processes, as they are manifested in ionospheric predictive capabilities in the intermediate and long-term temporal regimes (Szuszczewicz *et al.*, 1988; Schunk and Szuszczewicz, 1988; Spiro *et al.*, 1988; Robinson *et al.*, 1988; Leitinger *et al.*, 1988; Wilkinson *et al.*, 1988; Abdu *et al.*, 1988). For intermediate term processes, the SUNDIAL approach stresses the application of first principle modelling (Szuszczewicz *et al.*, 1988; Schunk and Szuszczewicz, 1988; Spiro *et al.*, 1988), while the emphasis is on empirical models for handling predictions in the longer term (Szuszczewicz *et al.*, 1988; Schunk and Szuszczewicz, 1988). Efforts are also directed at adaptive time-dependent empirical model development for application to intermediate term predictions. In intermediate and long-term cases, an acquired solar-terrestrial database provides the benchmarks against which the models are tested and improved to meet the program objectives. The SUNDIAL program has emphasized the first principle codes generally referred to as the Rice Convection Model (Spiro *et al.*, 1988), the Utah State University (USU) ionospheric model (Schunk and Szuszczewicz, 1988), and the NCAR General Thermospheric Circulation Model (GTCM) (Roble *et al.*, 1988), while the empirical emphasis has

been on the International Reference Ionosphere, the IRI (Schunk and Szuszczewicz, 1988; Rawer, 1981).

The ionospheric monitoring network that supports the SUNDIAL effort involves nearly 70 stations covering high-, middle-, and low-latitudes in the American, European/African and Asian/Australian sectors. The ground-based ionospheric measurement techniques include ionosondes, backscatter radars, polarimeters, magnetometers, scintillation receivers, all-sky and scanning photometers, and Fabry-Perot interferometers, with some site-specific capabilities presented in Szuszczewicz *et al.* (1988). The program operates with an agreement on common data formats and works to accomplish around-the-clock data collection on a minimum-resolution quarter-hourly basis for campaign periods 8-30 days in length. Solar data and geomagnetic indices are provided through the National Oceanographic and Atmospheric Association (NOAA), while the properties of the interplanetary medium are obtained from the principal investigators for relevant sensors on IMP-8 (R. Lepping, IMF; and J. Gosling, solar wind plasma) and from published results in Solar Geophysical Data issued by the NOAA National Satellite Data and Information Services.

The first SUNDIAL modelling and measurement campaign concentrated on the interval 5-13 October 1984, a time that approached solar minimum in the declining phase of Solar Cycle 21. The observations and analyses covered the coupling of processes from a trans-equatorial coronal hole through the interplanetary and magnetospheric domains down to the equatorial ionosphere, where penetrating electric fields triggered the most disturbed condition of equatorial spread-F ever recorded by the Jicamarca Observatory (Szuszczewicz *et al.*, 1988; Spiro *et al.*, 1988). The correlation of events also included: (1) enhanced particle precipitation at high latitudes, (2) an associated cross polar cap potential of 75 kV, and (3) simultaneous globally-enhanced F-region dynamics.

Analysis of the 1984 results also considered the « quiet », « disturbed » and « averaged » conditions of the global-scale F-region ionosphere, with a special emphasis directed at the « quiet » and « averaged » conditions (Leitinger *et al.*, 1988; Wilkinson *et al.*, 1988; Abdu *et al.*, 1988). Concentrating on the diurnal behavior of the peak F_2-region densities (N_mF_2), comparisons were made among the SUNDIAL data and the IRI and USU models. In the USU model the input parameters (electric fields, neutral winds, etc.) were selected to represent a simple « averaged » condition for the time of observation. During daytime periods the IRI matched the averaged mid-latitude N_mF_2 diurnal behavior quite well; and the IRI was better than the USU model in this regard. The IRI also agreed well with the averaged observations during the nighttime periods, while the disagreement between observations and the USU predictions grew worse. For all mid-latitude stations, the USU results underestimated the values for N_mF_2 between midnight and dawn, and in most cases the underestimate was severe (typically differences involved factors of 2-3).

The IRI also out-performed the USU model at low and equatorial latitudes. The USU results continued

to underestimate the nighttime values for N_mF_2, and incorrectly displayed a temporal displacement of the peak daytime value of N_mF_2. Typically, observations of the N_mF_2 daytime peak occurred between 14 and 16 h LT, whereas the USU results predicted the occurrence of the daytime peak some 2 to 3 h later. It is believed that these discrepancies, as well as those at mid-latitudes, were a result of an oversimplified specification of thermospheric winds and global electric fields in the USU code. This problem of winds and electric field specification confronts the entire ionospheric community. In the 1984 effort, the USU model only considered the meridional component of the thermospheric wind, prescribing a maximum value of 200 m/s at night and a minimum of 0 m/s during the day (Szuszczewicz et al., 1988; Wilkinson et al., 1988), with an associated latitudinal and longitudinal distribution described in Sojka and Schunk (1985). On the issue of electric fields, the USU code employed the electric field model of Richmond et al., 1980. While that electric field model was intended to be global, it is based only on data collected near the 75° W longitude, and the data were seasonally-averaged. It represented an important first step in specifying the global-scale ionospheric electric field distribution but a more accurate specification is required if advances are to be made in ionospheric modelling and predictability. The work of Wilkinson et al. (1988) helped highlight this issue and brought focus on the need for follow-up activities. Some of that work has been undertaken by Fejer et al. (1990).

Since the 1984 effort the USU model has undergone additional testing, with specific comparisons against the SUNDIAL data acquired during the 1986 campaign (Sica et al., 1989). In this most recent effort, the USU results were found to match averaged results of 41 mid-latitude ionosonde stations with the neutral meridional wind as a free parameter. The meridional wind required to fit the data was consistent from location to location and with previous neutral wind measurements and models. The effort also drew attention to the general lack of knowledge of O^+ flux variations in the topside ionosphere and the influence of that parameter on the uncertainty in deduced thermospheric winds.

The assets and inadequacies of the IRI model were also highlighted in the 1984 SUNDIAL effort. The IRI is a simple, fast-running PC-compatible code that allows a synthesized perspective on UT, LT, solar-cycle, seasonal and magnetic latitude effects on electron densities, ion composition and plasma temperatures from 80 to above 1000 km. The SUNDIAL investigation treats the IRI as an evolutionary code with the expectation that comparisons of theoretical predictions and experimental results with the IRI will be useful in providing an improved prescription of the global-scale ionosphere and an adaptive model specification which will allow descriptions of global ionospheric responses to such dynamic events as magnetic storms. As the IRI is the most tested global-scale empirical ionospheric model in a fast running PC format, it represents an excellent baseline upon which to develop a time-dependent adaptive ionospheric model. It also provides a convenient, computer-effi-

cient format for comparing global-scale results and attempting their interpretation in terms of latitudinal and longitudinal coupling. It is with this perspective that the IRI continues to have the attention of the international community and the SUNDIAL investigation.

In this work we establish several new perspectives on the IRI. The first attempts to mitigate its shortcomings in specification of the high latitude ionosphere. While our current effort does not include the actual enhancements in high latitude ionization brought about by energetic particle precipitation, we include an empirical model for auroral oval boundaries and incorporate the associated specifications of high-latitude phenomenology into our interpretation of results. We focus on the latest campaign results, collected during September 1986. Our treatment of these data and its comparisons with the IRI are intended as the first step to the development of an adaptive model which can empirically track the dynamics of the global-scale ionosphere from quiet to disturbed conditions, regardless of the time, disturbance level and position within the solar cycle. This is a step away from the « monthly-averaged » IRI specification towards a time-dependent « disturbance-sensitive » model for intermediate and longer term predictions.

2. PREVAILING SOLAR-TERRESTRIAL CONDITIONS

The SUNDIAL-86 campaign covered 22 September through 4 October 1986, a period that coincided with the very extreme of solar minimum. The entire month of September was free of solar activity and the sunspot number was zero during most of the period. (See synoptic presentation of solar-terrestrial indices in Fig. 1.) For several months up to and through September, geomagnetic activity and solar wind plasma characteristics demonstrated a clear 27 day recurrence. The recurring stream first appeared on 27 June (day 177), and reappeared every 27 days through 13 October (day 286). In subsequent months the high speed stream was gone, phenomenological evidence of changing solar morphologies as the Sun entered its ascending phase. The streams were characterized by plasma density enhancements on the leading edge and elevated plasma temperatures behind. The interaction of these streams and their associated interplanetary fields triggered a transition in geomagnetic activity from a quiet ($K_p = 0$ to 2) to a disturbed ($K_p = 4$ to 6) state.

While recurring high-speed solar wind streams bracketed the SUNDIAL campaign period, the SUNDIAL-86 stream was non-recurrent, and therefore evolved on a timescale of a solar rotation. The plasma signatures of the SUNDIAL stream were identical to those of the recurring streams; that is, it was characterized by an increased velocity, an enhanced density peak on its leading edge, and elevated temperatures behind. The plasma data for the SUNDIAL stream is presented in Figure 2, with its corresponding K_p characteristics in Figure 1 showing a transition from 0 and 0+, to 5 and 6.
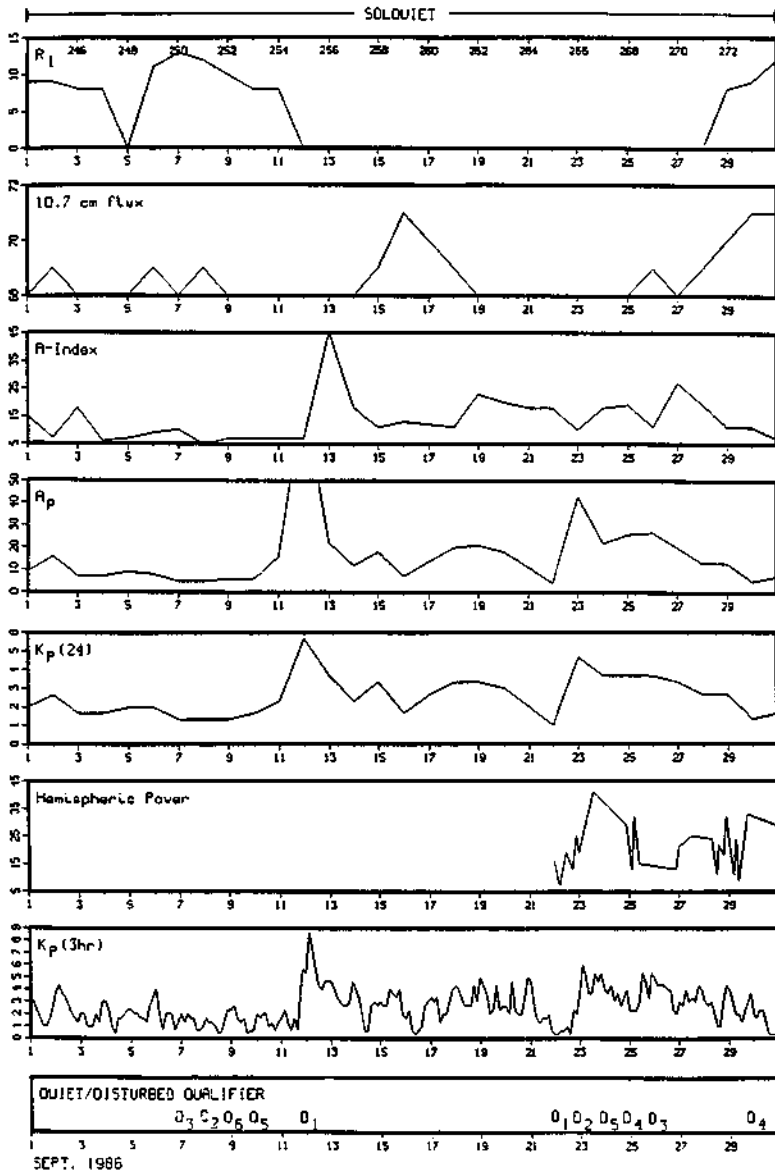
Figure 1

Composite representation of prevailing solar-terrestrial conditions during September 1986. Top-to-bottom panels include : the international sunspot number R_I, the 10.7 cm flux, the A-index, the planetary A_p index, the 24 h planetary K_p index, the NOAA/TIROS hemispheric power, the 3 h average K_p, and the quiet/disturbed day qualifier (Q_1 = most quiet day, D_1 = most disturbed day).
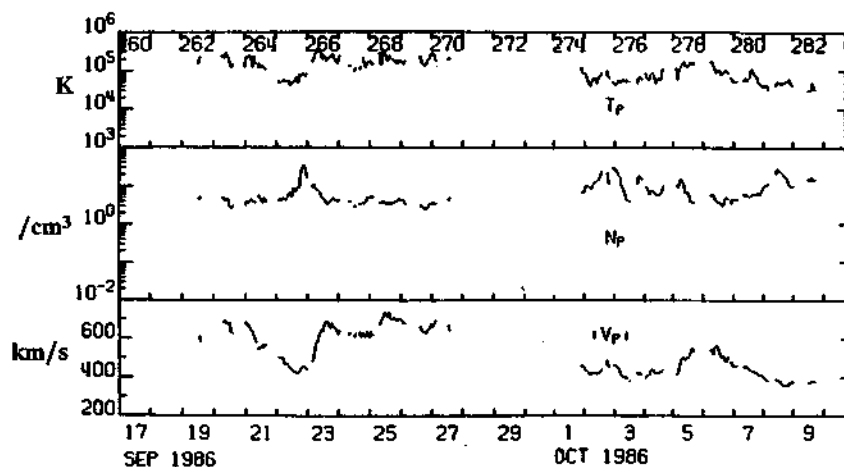

Figure 2

IMP-8 solar wind plasma parameters measured during the SUNDIAL-86 campaign interval (22 Sept.-4 Oct. 1986). Note high-speed stream and density enhancement on leading edge late on 22 September.

As suggested by the K_p values in Figure 1, as well as the A_p indices and the NOAA/TIROS measurements of hemispheric power (Szuszczewicz *et al.*, 1988 ; Foster *et al.*, 1986) also presented in Figure 1, the first 20-21 h of 22 September were very quiet (rated Q1),

the 23-26 September period was substantially disturbed (rated D2-D5), and the remaining days of the campaign calmed monotonically to a K_p = 0 day late on 30 September.

The transition from the Q1 condition on 22 September to the D2-D5 conditions on 23 through 26 September was also manifested in the B_z-component of the IMF which we present in Figure 3. The data show that B_z was effectively zero from 0 to 19 UT on 22 September. At 1920 UT there was a 20 min southward turning of the IMF, followed by a mostly northward configuration (arguable because of IMF data gaps) into the very early morning of 23 September. B_z

variations on the 23rd displayed dynamic N-S oscillations and drifted toward a quieting behavior on the 24th and 25th. We note that the brief southward turning of the IMF at 1920 UT on the 22nd is coincident with the positive slope in density enhancement at the leading edge of the SUNDIAL stream and that the IMF dynamics during 23-25 September occur within the body of the high speed stream behind the enhanced density front.
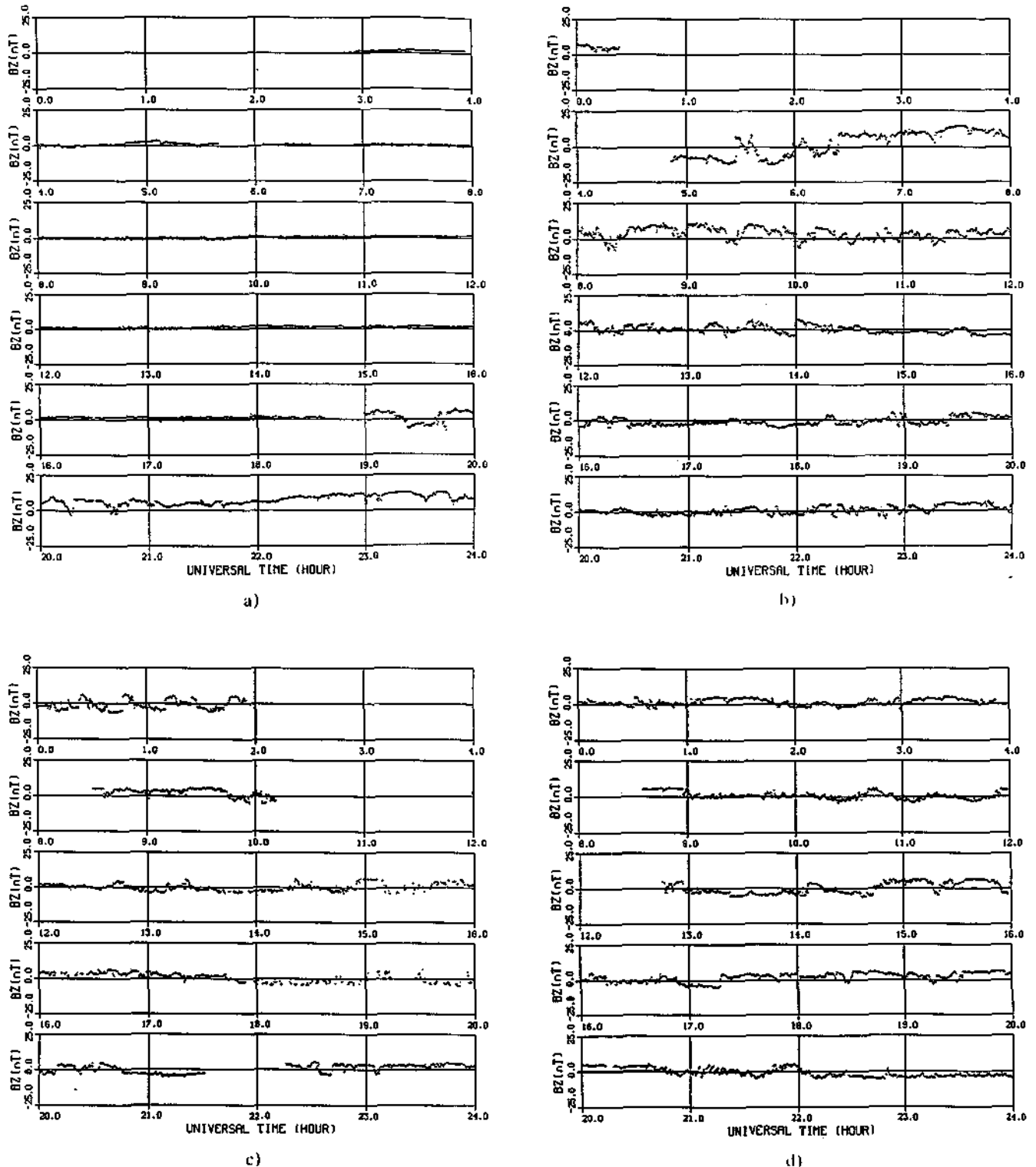

Figure 3

Z-component of the interplanetary magnetic field for (a) 22 September, (b) 23 September, (c) 24 September, and (d) 25 September 1986 (from R. Lepping).

The manifestations of the interplanetary dynamics in IMF and solar wind characteristics were clearly displayed in the Kiruna magnetograms presented in Figure 4. The brief southward excursion of the IMF at 1920 UT and the solar wind density enhancement at its leading edge appear to be directly correlated with the small enhancement in the *x*-component of the magnetogram just before 20 UT on 22 September. Nearly coincident with this was a brief 20 min interval of radar backscatter at SABRE in the Northern European sector (~ 21 UT), suggesting an enhancement in the high-latitude convection (M. Lester, private communication). We note also that the IMF and high speed stream dynamics on the 23rd have their cause-effect counterparts in the magnetogram data on the same day.

3. IONOSPHERIC EVENTS, GLOBAL MEASUREMENTS AND MODEL COMPARISONS

Overall ionospheric responses have been found to correlate well with the solar, interplanetary and geomagnetic conditions described in the previous section. This is illustrated in the 1986 event synopsis chart in Table 1 which covers the full SUNDIAL period and lists observational descriptives from a number of the SUNDIAL participants. The NOAA data reported by J. Joselyn indicated that magnetic storm conditions began at about 1900 UT on 22 September, ending about 23 UT on the 24th. The magnetic storm onset time and subsequent periods of disturbance indicated by the NOAA data agrees
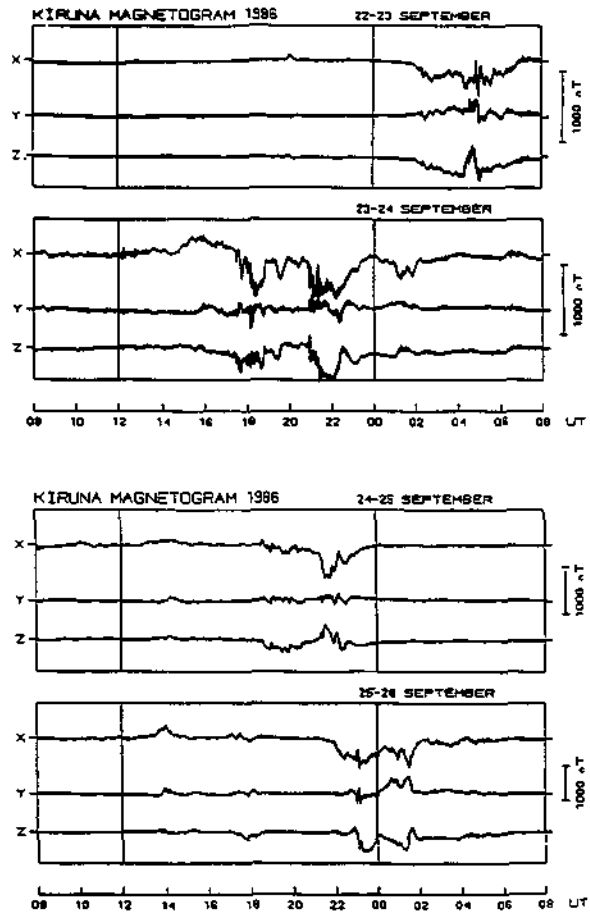

Figure 4

Kiruna magnetograms for the period 22-26 September, 1986 (from G. Gustafsson).

Table 1

SUNDIAL-86 *event synopsis.*

SUNDIAL/IRI
Comparison of Sundial to IRI FOF2 (MHz) values for Sept. 22 - Sept. 30 1986
Feldstein Oval Model
UT- 0   R- 10.0   Q-6

255.0 mlg	349.0 mlg	75.00 mlg	165.0 mlg
71.5 mlat	66.2 mlat	62.9 mlat	66.7 mlat
12.0 mlt	18.0 mlt	0.00 mlt	6.00 mlt

noon   midnight   noon

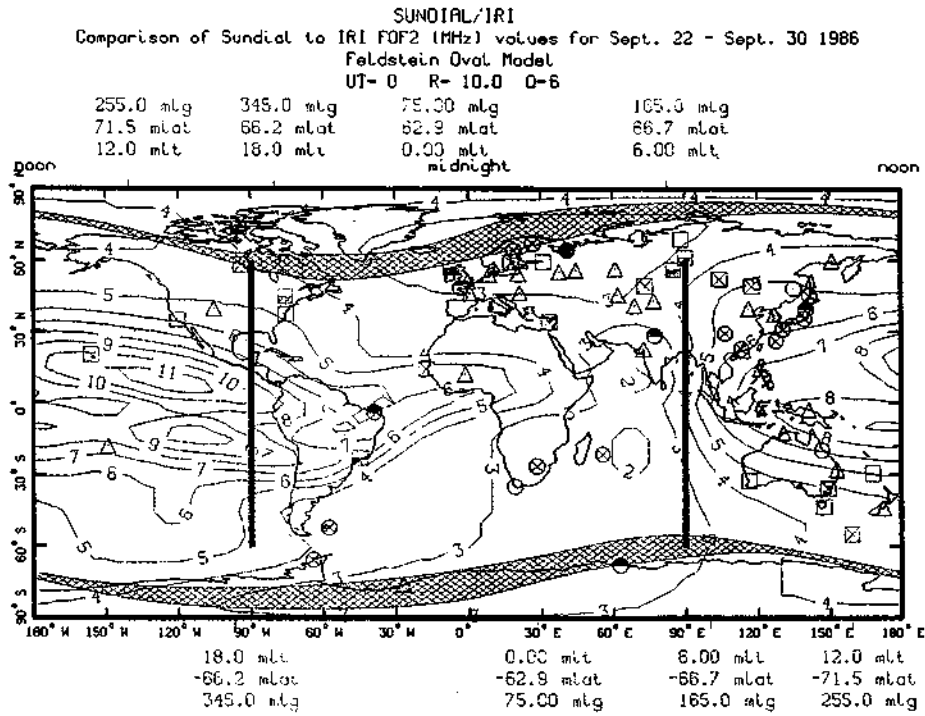| 18.0 mlt | 0.00 mlt | 6.00 mlt | 12.0 mlt |
| -66.2 mlat | -62.9 mlat | -66.7 mlat | -71.5 mlat |
| 349.0 mlg | 75.00 mlg | 165.0 mlg | 255.0 mlg |

Figure 5

Global maps of IRI *contours (for September, solar-minimum,* UT = 0) *of* f_oF_2 *(green contours in* MHz), *with Feldstein* Q = 6 *oval. Symbols identify* SUNDIAL *stations with 8-day-averaged values of* f_oF_2 *observations at* UT = 0. Δ's *specify agreement within* ± 5 %, *while* □, ⊠, ▣, *and* ■ *indicate that the observations are less than* IRI *specifications by* 5-10 %, 10-20 %, 20-40 % *and* > 40 %, *respectively.* O, ⊗, ◓, *and* ● *have the same quantitative scaling but for observations greater than the* IRI *specifications. Vertical line identifies the sunrise and/or sunset terminator.*

SUNDIAL/IRI
Comparison of Sundial to IRI FOF2 (MHz) values for Sept. 22 - Sept. 30 1986
Feldstein Oval Model
UT- 6   R- 10.0   Q-6

248.0 mlg	338.0 mlg	68.00 mlg	158.0 mlg
66.1 mlat	62.8 mlat	66.8 mlat	71.5 mlat
18.0 mlt	0.00 mlt	6.00 mlt	12.0 mlt

midnight   noon

0.00 mlt	6.00 mlt	12.0 mlt	18.0 mlt
-62.8 mlat	-66.8 mlat	-71.5 mlat	-66.1 mlat
338.0 mlg	68.00 mlg	158.0 mlg	248.0 mlg
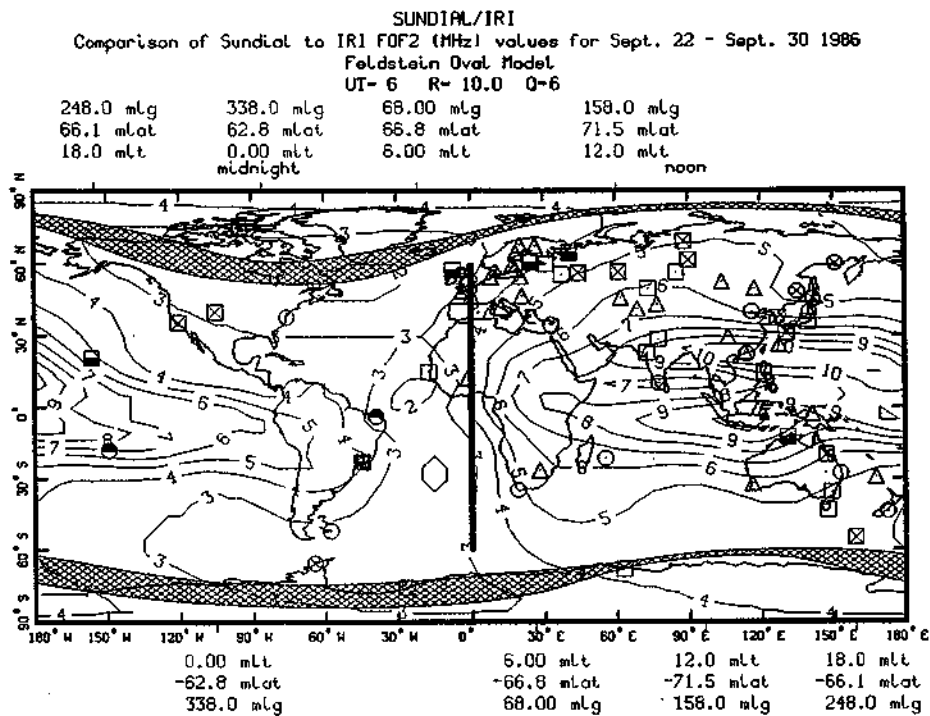
Figure 6
Same as Figure 5 but UT = 6.

SUNDIAL/IRI
Comparison of Sundial to IRI FOF2 (MHz) values for Sept. 22 - Sept. 30 1986
Feldstein Oval Model
UT-12   R- 10.0   O-6

246.0 mlg	336.0 mlg	66.00 mlg	156.0 mlg
62.9 nlat	66.8 mlat	71.5 mlat	66.1 mlat
0.00 mlt	6.00 mlt	12.0 mlt	18.0 mlt
midnight		noon	midnight

6.00 mlt	12.0 mlt	18.0 mlt	0.00 mlt
-66.9 mlat	-71.5 mlat	-66.1 mlat	-62.9 mlat
336.0 mlg	66.00 mlg	156.0 mlg	246.0 mlg
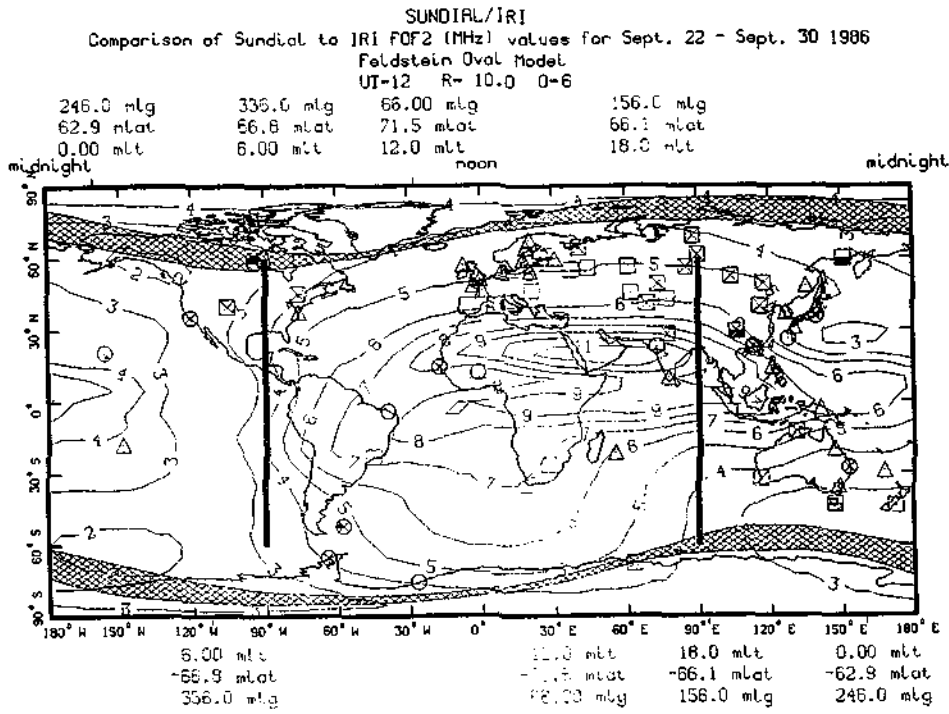
Figure 7
Same as Figure 5 but UT = 12.

SUNDIAL/IRI
Comparison of Sundial to IRI FOF2 (MHz) values for Sept. 22 - Sept. 30 1986
Feldstein Oval Model
UT-18   R- 10.0   O-6

252.0 mlg	342.0 mlg	72.00 mlg	162.0 mlg
66.8 mlat	71.5 mlat	66.1 mlat	62.9 mlat
6.00 mlt	12.0 mlt	18.0 mlt	0.00 mlt
	noon		midnight

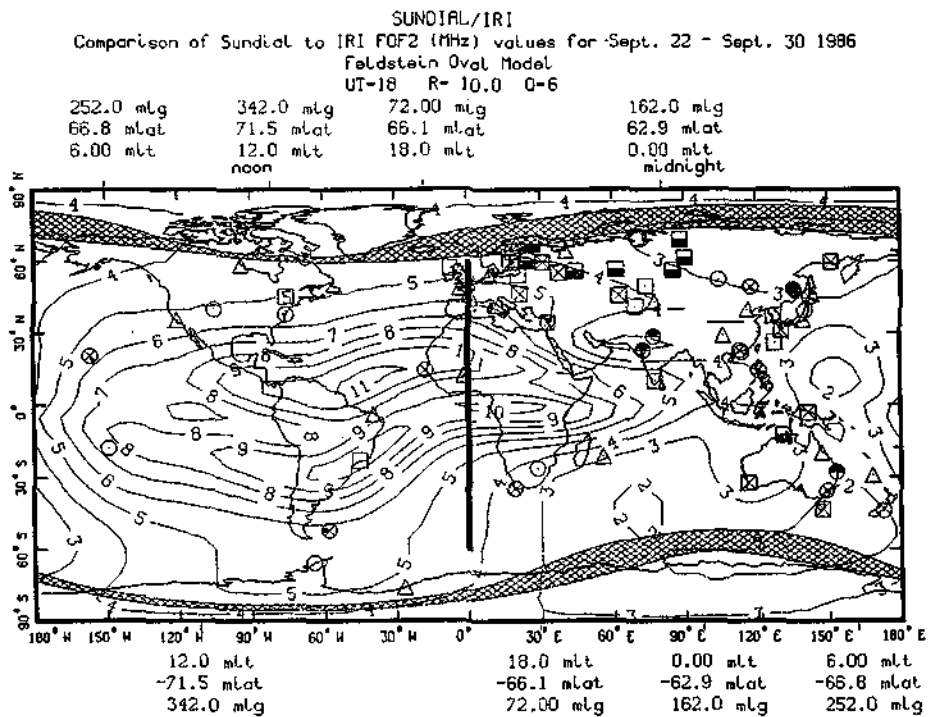| 12.0 mlt | 18.0 mlt | 0.00 mlt | 6.00 mlt |
| -71.5 mlat | -66.1 mlat | -62.9 mlat | -66.8 mlat |
| 342.0 mlg | 72.00 mlg | 162.0 mlg | 252.0 mlg |

Figure 8
Same as Figure 5 but UT = 18.

394

reasonably well with the ionospheric observations of Inuke in the Japanese sector, Abdu in the South American sector, and with the Northern Hemisphere observations compiled by Wilkinson. The Millstone Hill (J. Foster) and Sondrestrom (de la Beaujardiere) radars reported storm-related events on the 23rd, 24th and into the 25th, including enhanced convection and large ion drift velocities. Coordinated observations with the VIKING satellite (Gustafsson) showed images of complex auroral ovals, including a surge in the Sondrestrom field of view. In terms of quiet-day specifications, Walker's results in the Asian sector point to 22 September as the quietest day, while Wilkinson and Abdu point to 1 October. All observations show the 23-25 September period as the most disturbed, with some quantitative differences in the longitudinal chain and in the Northern and Southern Hemispheres (e.g. Wilkinson).

In this paper, we focus on ionosonde observations of peak F_2-region electron densities at 0, 6, 12 and 18 UT averaged over the 22-30 September period. The results are presented in Figures 5 through 8, against a background of f_oF_2 contours from the IRI $(f_oF_2 \text{ [mHz]} = 8900 \sqrt{(N_mF_2 \text{ [cm}^{-3}])})$. Qualitatively and quantitatively IRI contours have been found to provide a good representation of diurnal F-region behavior when compared with monthly-averaged topside sounder data near solar maximum (Schunk and Szuszczewicz, 1988). However, the case in hand is that of solar minimum, and the comparison to be presented is thought to be the first in a global format.

We note that the f_oF_2 contours in Figure 5 provide clear perspectives on major ionospheric morphologies. The equatorial anomaly (see e.g. Walker and Strickland, 1981) appears in the noon to early afternoon period, with peak densities in the anomaly occurring between 14 and 16 h LT, and with the latitudinal symmetry axis of the anomaly tracking the geomagnetic dip equator. The contours show a nighttime collapse in f_oF_2 with the lowest values in the mid- and equatorial latitude domains occurring near 0400 LT. Values of f_oF_2 are seen to increase near the sunrise terminator at 0600 LT and develop the early sunrise enhancement in F-region densities as expected intuitively. The sunrise and sunset terminators in Figure 5 are marked with vertical lines.

At auroral latitudes the IRI is frequently criticized for its inadequate specification of the ionosphere. We note however that in its monthly-averaged format, the IRI agrees quite well with the high-latitude monthly-averaged f_oF_2 observations of the ISSB satellite (Schunk and Szuszczewicz, 1988). This is because the process of monthly averaging tends to smear-out the influences of particle-enhanced ionization levels and depletions in the mid-latitude trough. On a non-averaged basis however, it is clear that both particle enhancements and trough depletions need to be taken into account. The addition of an empirically-based auroral oval can mitigate this concern with the IRI at high-latitudes. To this end we have conducted a review and comparison of several empirically-derived auroral-oval models, including the Feldstein, 1963, DMSP (Hardy et al., 1985, 1987) and NOAA/TIROS

ovals (Foster et al., 1986; T. Fuller-Rowell and D. Evans, private communication) for addition to the SUNDIAL IRI. The NOAA/TIROS prescription appears to be the most promising for future applications, due in part to the fact that the NOAA/TIROS model includes an empirical specification of convection patterns that are consistent with the ovals and tunable to prevailing geomagnetic conditions. Like the DMSP oval model it is also updatable on an orbit-to-orbit basis, and can lend itself to adaptive modelling techniques. Unfortunately it has yet to be tested against an independent data set in order to establish its accuracy in a global specification of oval boundaries. This is also true of the DMSP model.

With both DMSP and NOAA/TIROS models based on in situ particle data there is also some subjectivity in the definition of the poleward and equatorward boundaries. With these concerns we have elected to make use of the Feldstein oval (Feldstein, 1963; Holtzworth and Meng, 1975) in our analysis of data in Figures 5 through 8. The Feldstein oval is also more widely known and used. The most significant consequence of this choice and potential impact on the analysis of our results is that the equatorward boundaries of the Feldstein oval tend to be more poleward than those of the DMSP and NOAA/TIROS models (Sands and Szuszczewicz, unpublished). We have selected the $Q = 6$ magnetic activity level (approximately equivalent to $K_p = 4$) in order to represent a Feldstein oval configuration under moderately disturbed conditions. We estimate this to be a reasonable approach in our comparisons with the conditions averaged over the 22-30 September period.

We turn now to the f_oF_2 ionosonde results and their representation in Figure 5. The symbols are located at each station where observations were available. The triangles represent agreement (within 5 %) between the observation and the IRI value, while circles (squares) represent higher (lower) observations than those specified by local IRI values. As the symbols become filled (first with an « x », then half filled, and finally completely filled) the disagreement increases from 5-10 %, to 10-20 %, to 20-40 %, and finally to > 40 %. The largest levels of disagreement are represented by blue circles and red squares.

Reviewing the contents of Figure 5 (UT = 0 h) we make the following observations: (i) There is excellent agreement (± 5 %) in the northern European sector in the midnight and post-midnight period. This same excellent agreement continues over the Soviet Union and into parts of Asia as the local time advances toward dawn. The good agreement extends to high mid-latitudes, up to the equatorward boundary of the post-midnight oval and into the region typically identified as the main nighttime trough. (ii) With local times near dawn in the Northern Hemisphere, the observations are lower than those specified by the IRI, with the disagreement not worse than about 30 %. (iii) In the early-to-mid morning hours in the Australian-longitude sector we find an interesting anti-symmetry between the Northern and Southern Hemispheres. The observations tend to be 10-20 % higher than the IRI in the Northern Hemisphere and 5-20 % lower than the IRI in the Southern Hemi-

sphere. This trend is also found to conform to the observation that the near-equatorial stations in this sector (Hong Kong to North Australia) meet the criterion for agreement within 5 %. (iv) At North and South American longitudes observations are relatively sparse in covering the sunset terminator in North America and a time frame near 2200 LT on the coast of Brazil. While low station density at these longitudes minimize the possibility to identify trends, we note that the observations generally fall in the 5-40 % range. We also note that the two observations in the northern oval ($\approx 60°$ N, 95° W) and cap ($\approx 80°$ N, 95° W) are no cause for alarm with respect to the merits of the IRI in this region. Similarly we point to the observation within the oval in the Southern Hemisphere at about (30° W, 80° S) and (60° E, 60° S). Those observations meet the 5 % and 20-40 % agreement criteria respectively. (v) Overall, we find good agreement between the observations and the IRI predictions under solar-minimum equinox conditions, at UT = 0 and with a Q = 6 Feldstein oval.

The data and IRI model contours for UT = 6 are represented in Figure 6, where the morphological features of the post-midnight collapse, the sunrise enhancement and the equatorial anomaly are evident and shifted appropriately in time when compared against Figure 5. Starting with the sunrise terminator (in this case the Greenwich meridian) we can advance the following observations : (i) The first two hours in the sunrise period above Europe show excellent agreement between the model and our observations. Similar comments can be made about the same time period over southern Africa, although the poor station density renders that an arguable conclusion ; (ii) As we move toward noon in the Northern Hemisphere, the higher latitude stations show lower f_oF_2 values than those of the IRI, with differences primarily in the 5-20 % range. By way of contrast, the lower mid-latitude sites in this same time zone are in ± 5 % agreement with the model specification. (iii) In the post-noon period we find the maximum density contours of the equatorial anomaly over the Asian-Australian sector, where the north-south asymmetry discussed in Figure 5 also seems to be in evidence. This is particularly true during LT = 0200-0400 h. The asymmetry (higher observed values in the Northern Hemisphere (compared with the IRI) than in the Southern Hemisphere) is not as convincing as in the UT = 0 case, but the preponderance of data at UT = 6 does support the asymmetry conclusion. (iv) The post-sunset through post-midnight station density is sufficiently thin to preclude descriptions of trends, but the results do not suggest any concern about major discrepancies. Most of the data in this time zone are in the 10-30 % regime with the exception of Cauchiera Paulista near Brazil's southern coast, where the observation fell into the greater than 40 % category. This is the only such large discrepancy in all our findings.

Figure 7 presents the data and IRI contours for comparison at UT = 12. We make the following observations : (i) At 1200 ± 0200 LT (centered on the Greenwich meridian), we find excellent agreement in the Northern Hemisphere, particularly over northern

Europe. The data over South Africa in this time zone are less than that of the IRI, but the disagreement is not worse than 5-10 %. (ii) The agreement in the Northern Hemisphere is still good (5-10 %) in the Soviet sector at 0200-0400 LT, but it grows to the 10-20 % level at and within 2 h of the sunset terminator. (iii) In the pre-midnight sector at Australian longitudes we find continued evidence for the north-south asymmetry discussed for earlier UT's, but the case here is arguable.

In Figure 8 we complete our comparison between observations and model specification focusing on UT = 18 h. In reviewing the content of that figure we draw the following conclusions : (i) The sunset terminator is at the Greenwich meridian, and the dominating observation is the disagreement between measurements and model predictions in the entire Northern Hemisphere between the sunset terminator and the midnight meridian. There appears to be no counterpart to this observation in the Southern Hemisphere. This conclusion is muted by the fact that the Southern Hemisphere stations are few in number and generally at lower latitudes than their northern counterparts. (ii) In the midnight-to-sunrise sector the results are mixed. Generally, the observations in the Northern Hemisphere tend to be higher than the IRI values, whereas just the opposite conclusion can be made with the same comparison in the Southern Hemisphere. The issue of clear north-south asymmetry is softer in our UT = 18 observations. (iii) In the western hemisphere, with noon centered over North America, the observations are distributed over the sunrise enhancement and on the poleward edges of the equatorial anomaly. These observations tend to be 5-15 % higher than those specified by the IRI. In this time frame (UT = 18) only the Brazilian station at Cauchiera Paulista is positioned at the anomaly peak, showing a value 5-10 % lower than that of the IRI.

4. COMPARISONS IN MAJOR PHENOMENOLOGICAL DOMAINS

In synthesizing our results, we focus on well-defined phenomenological domains (e.g. oval, trough, anomaly, etc.). We start with high-latitudes, a region where the IRI has been criticized. In addressing this issue we divide « high-latitudes » into (i) high mid-latitudes, in order to include the mid-latitude trough, (ii) the diffuse auroral oval, to include commentary on particle-produced ionization enhancements, and (iii) the polar cap, to include some discussion on F-region phenomena poleward of the auroral oval. We use the Feldstein model to define the oval (for Q = 6, as discussed previously), the polar cap, and the poleward boundary of the mid-latitude trough. Admittedly, the oval model represents an averaged prescription tuned to a prevailing geomagnetic condition. But it is in this spirit of « averages » that the comparisons are being made. The IRI is monthly averaged, and our ionospheric data have been averaged over the SUNDIAL campaign period.

At the present time the SUNDIAL network has few stations that provide coverage of particle-enhance-

ment ionization in the diffuse oval (at UT = 0, 6, 12 and 18 h), but of those providing f_oF_2 data during the 1986 campaign (see Figs. 5-8), the agreements between observations and the IRI values were generally good, and certainly not worse than our findings at mid- and equatorial-latitudes. Two issues favor the agreement within the diffuse oval at F-region altitudes : (1) the averaging process itself, and (2) precipitating particles in the oval deposit the bulk of their energy (and ionizing effects) below the F_2-peak.

The paucity of stations in the polar cap region is also of concern when drawing conclusions relevant to that domain. But working with available measurements during SUNDIAL-86 we find the agreement between observations and model predictions generally in the 10-30 % range, again no worse than our accumulated findings at mid- and equatorial-latitudes. For the phenomenologies active in the polar cap, it is likely that first principle codes will not give better estimates of the F_2-peak behavior than the IRI, since the behavior is driven by photo-ionization, soft-particle precipitation (« polar rain »), convection of long-lived O^+ « blobs », and broad spectral distributions of density irregularities redistributed throughout the polar cap (Szuszczewicz, 1984). Convective transport and long-lived irregularities can dominate the polar cap (particularly regions without photoionization) and result in an inordinate complication in a first-principle code approach to prediction.

Relative to the trough region, we define it to have a width of $7°-10°$, with a minimum density centered near local midnight at MLAT = $60°$. Electron content data measured during the SUNDIAL-86 campaign support this but with the suggestion that trough widths at solar minimum may be as large as $12°-14°$ (R. Leitinger, private communication). We also assume that the east-west morphology of the trough extends from the late afternoon to the sunrise terminator. This defi--nition of the trough is in reasonable agreement with earlier observations and theoretical descriptions (Evans et al., 1983 ; Tulunay and Grebowsky, 1975 ; and Spiro et al., 1978) although several observations in the European sector near local noon suggest trough-like features (Lester et al., 1990). For purposes of discussing the relevant results in Figures 5-8, we consider the domain of the trough to occupy a $7°$ to $10°$ band equatorward and adjacent to the oval extending from the dusk period to the sunrise terminator. The best time frames to render a meaningful comparison with SUNDIAL data are at UT = 0 (Fig. 5) and UT = 18 (Fig. 8). At UT = 0, the data density is good, and the ionosonde results show what appears to be a trough above northern Europe, where we see « depletions » (boxes) located at a nominal trough position bracketed on the north by « enhancements » (circles) and on the south by observations that match the IRI perfectly ($\pm$ 5 %). Looking for possible corroboration, we turn to the post-sunset through midnight period at UT = 18 (Fig. 8), and see a preponderance of « depletions » (boxes) at northern high latitudes. However, it is impossible to identify those depletions with the trough since the observed « depletions » have a $30°$ latitudinal spread. This is not a trough characteristic. We also note that the prepon-

derance of data in the Soviet sector shows values less than that specified by the IRI. This is clear at UT = 6, 12 and 18, suggesting that modifications to the IRI in this region have more to do with improving its underlying data set than with its ability to track the trough.

We turn our attention to the sunrise and sunset terminators and offer the following observations : (i) If there is an effect to be seen, it is at UT = 0, at high mid-latitudes over the Soviet Union. The data show a reduction in the values of f_oF_2 below those specified by the IRI at a time that coincides with 0600 $\pm$ 0200 h LT. Inspection of the results near the terminators at other UT's does not provide convincing support that the SUNDIAL-86 data suggest modification in IRI specification of f_oF_2 contours at and near the terminators. We conclude that there is need for additional work, and that the current data do not allow a definitive conclusion.

We turn now to the apparent asymmetry between the Southern and Northern Hemispheres at Australian longitudes. This asymmetry was most convincing at UT = 0 with LT = 0630-1200 h. It is also supported at UT = 6 h (LT = 1400-1700 h) in the same geographic region, and with somewhat lessening conviction at UT = 12 h. The result does not suggest a flawed IRI specification of the sunrise enhancement or post-noon anomaly at higher mid-latitudes in the Australian-Japanese sector, but it does suggest that improvements can be made by increasing the empirical base upon which this region of the IRI was developed. At the moment the data suggest that the IRI contours in the Northern Hemisphere should be decreased 10-20 %, while those in the Southern Hemisphere need to be increased 5-15 %.

5. FINAL COMMENTS

Overall, we find good agreement between the IRI and the SUNDIAL-86 observations of the F-region ionosphere averaged over an 8-day equinoctial solar-minimum period under moderately disturbed conditions. We have added a specification of the auroral oval, having reviewed the DMSP, Feldstein and NOAA/TIROS models. Our current assessment of the IRI's representation of F_2 peak densities at high, middle and equatorial latitudes suggests that under averaged solar-minimum equinoctial conditions major modifications are not necessary, since the contours are in reasonable agreement with our observations. We verify also that on the average the model provides a reasonable specification of the mid-latitude trough and the equatorial anomaly.

This effort focused on averaged responses during a solar-minimum equinoctial campaign. Future efforts will be directed at comparisons against additional SUNDIAL campaign data sets covering both equinoctial and solstitial periods with progressively increasing sunspot numbers (see campaign schedule in Szuszczewicz et al., 1988). These efforts will work to include modification of the IRI for its development as a time-dependent adaptive empirical model, capable

of specifying the transition of the global ionosphere from a quiet to a disturbed condition. The SUN-DIAL-86 data are expected to provide an initial opportunity to do this with further analysis of the accumulated observations. The conditions appear to be well suited, having started with a Q1 day and transitioning to a substantially disturbed state in response to a high speed solar wind stream. Some of this work based on the SUNDIAL-86 data has already been initiated in the investigations of Abdu *et al.* (1990), Lester *et al.* (1990), with Fejer *et al.* (1990)

studying the penetration of magnetospheric electric fields to low latitudes in response to changing interplanetary conditions. Important complementary efforts also include support studies of high-latitude convection patterns (Emery *et al.*, 1990) and thermospheric winds (Biondi *et al.*, 1990). The composite is expected to advance our understanding of the contributing forces of electric fields and thermospheric winds, and improve our overall predictive capability for the state and condition of the global-scale ionosphere.

REFERENCES

Abdu, M. A., B. M. Reddy, G. O. Walker, R. Hanbaba, J. H. A. Sobral, B. G. Fejer, R. F. Woodman, R. W. Schunk, and E. P. Szuszczewicz, Processes in the quiet and disturbed equatorial-low latitude ionosphere : SUNDIAL campaign 1984, *Ann. Geophysicae*, 6, 69-80, 1988.

Abdu, M. A., G. O. Walker, B. M. Reddy, J. H. A. Soabral, B. G. Fejer, T. Kikuchi, N. B. Trivedi, and E. P. Szuszczewicz, Electric fields *versus* neutral wind control of the equatorial anomaly under quiet and disturbed conditions : A global perspective from SUNDIAL-86, *Ann. Geophysicae*, 8, 419-430, 1990.

Biondi, M. A., J. W. Meriwether, Y. Sahai, and H. Takahashi, Thermospheric neutral winds at low latitudes during the September-October 1986 SUNDIAL campaign : Optical interferometer results, *Ann. Geophysicae*, 8, 409-418, 1990.

Emery, B. A., A. D. Richmond, H. W. Kroehl, C. D. Wells, J. M. Ruohoniemi, M. Lester, D. J. Knipp, F. J. Rich, J. C. Foster, O. de la Beaujardière, C. Senior, L. M. Shier, J. F. McKee, and S. Maeda, Electric potential patterns deduced for the Sundial period of September 23-26, 1986, *Ann. Geophysicae*, 8, 399-408, 1990.

Evans, J. V., J. M. Holt, W. L. Oliver, and R. H. Wand, The fossil theory of nighttime high-latitude F-region troughs, *J. Geophys. Res.*, 88, 7769-7782, 1983.

Fejer, B. G., R. W. Spiro, R. A. Wolf, and J. C. Foster, Latitudinal variation of perturbation electric fields during magnetically disturbed periods : 1986 SUNDIAL observations and model results, *Ann. Geophysicae*, 8, 441-454, 1990.

Feldstein, Y. I., On the morphology of auroral and magnetic disturbances at high latitudes, *Geomagn. Aeron.*, 3, 183-192, 1963.

Foster, J. C., J. M. Holt, R. G. Musgrove, and D. S. Evans, Ionospheric convection associated with discrete levels of particle precipitation, *Geophys. Res. Lett.*, 13, 656-659, 1986.

Hardy, D. A., M. S. Gussenhaven, and A. Huber, The precipitating electron delectors (SSJ/3) for the black 5D/flights 2-5 DMSP satellites : calibration and data presentation, *Rep. AFGL-TR-79-0216*, AFGL Hanscom AFB, MA, 1979.

Hardy, D. A., M. S. Gussenhoven, and E. Holeman, A statistical model of auroral electron precipitation, *J. Geophys. Res.*, 90, 4229-4248, 1985.

Hardy, D. A., M. S. Gussenhaven, R. Raistrick, and W. J. McNeil, Statistical and functional representations of the pattern of auroral energy flux, number flux, and conductivity, *J. Geophys. Res.*, 92, 12275-12294, 1987.

Holzworth, R. H., and C. I. Meng, Mathematical representation of the auroral oval, *Geophys. Res. Lett.*, 2, 377-382, 1975.

Leitinger, R., P. Wilkinson, and R. Hanbaba, The ionosphere in mid-latitudes during the SUNDIAL campaign, *Ann. Geophysicae*, 6, 59-68, 1988.

Lester, M., J. Foster, V. Wickwar, and G. Gustafsson, Multi-radar study of ionospheric trough dynamics during the Sundial-86 campaign, Submitted to *Ann. Geophysicae*, 1990.

Rawer, K., International Reference Ionosphere-IRI 79, NOAA Rep., UAG-82, U.S. Dept. of Commerce, Washington, D.C., 1981.

Rawer, K., and Y. V. Ramanamurty (eds.), International Reference Ionosphere-Status 1985/86. *Adv. Space Res.*, 5, 1985.

Richmond, A. D., M. Blanc, B. A. Emery, R. H. Wand, B. G. Fejer, R. F. Woodman, S. Ganguly, P. Amayenc, R. A. Benke, C. Calderon, and J. V. Evans, An empirical model of quiet day ionospheric electric fields at middle and low latitudes, *J. Geophys. Res.*, 85, 4658-4664, 1980.

Robinson, T. R., J. A. Waldock, M. D. Burrage, and T. B. Jones, High latitude ionospheric response to changes in the interplanetary medium : SABRE observations during SUNDIAL, *Ann. Geophysicae*, 6, 51-58, 1988.

Robinson, R. M., R. R. Vondrak, K. Miller, T. Dabbs, and D. Hardy, On calculating ionospheric conductances from the flux and energy of precipitating electrons, *J. Geophys. Res.*, 92, 2565-2570, 1987.

Roble, R. G., E. C. Ridley, A. D. Richmond, and R. E. Dickson, A coupled thermosphere/ionosphere general circulation model, *Geophys. Res. Lett.*, 15, 1325-1328, 1988.

Schunk, R. W., and E. P. Szuszczewicz, First-principle and empirical modelling of the global-scale ionosphere, *Ann. Geophysicae*, 6, 19-30, 1988.

Sica, R. J., R. W. Schunk, and P. J. Wilkinson, A study of the undisturbed mid-latitude ionosphere using simultaneous, multiple-site ionosonde measurements, *J. Geophys. Res.*, in press, 1989.

Sojka, J. J., and R. W. Schunk, A theoretical study of the global F-region for June solstice, solar maximum and low magnetic activity, *J. Geophys. Res.*, 90, 5285-5298, 1985.

Spiro, R. W., R. A. Heelis, and W. B. Hanson, Ion convection and the formation of the mid-latitude F-region ionization trough, *J. Geophys. Res.*, 83, 4255-4264, 1978.

Spiro, R. W., R. A. Wolf, and B. G. Fejer, Penetration of high-latitude-electric-field effects of low latitudes during SUNDIAL 1984, *Ann. Geophysicae*, 6, 39-50, 1988.

Szuszczewicz, E. P., High-latitude ionospheric plasma dynamics : Phenomenology, irregularity distributions transport and magnetospheric coupling, in *Solar-Terrestrial Physics : Present and Future*, NASA Ref. Publ. 1120, June 1984.

Szuszczewicz, E. P., B. G. Fejer, E. Roelof, R. Schunk, R. Wolf, R. Leitinger, M. Abdu, B. M. Reddy, J. Joselyn, P. Wilkinson, and R. Woodman, SUNDIAL : A world-wide study of interactive ionospheric processes and their roles in the transfer of energy and mass in the Sun-Earth system, *Ann. Geophysicae*, 6, 3-18, 1988.

Tulunay, Y. K., and J. M. Grebowsky, Temporal variations in the dawn and dusk mid-latitude trough positions, measured (ARIEL3, ARIEL4) and modelled, *Ann. Geophys.*, 31, 29-38, 1975.

Walker, G. O., and A. E. Strickland, A comparison of the ionospheric equatorial anomaly in the East Asian and the American regions at sunspot minimum, *J. Atmos. Terr. Phys.*, 43, 589, 1981.

Wilkinson, P. J., R. Schunk, R. Hanbaba, and H. Mori, Interhemispheric comparison of SUNDIAL F-region data with global scale ionospheric models, *Ann. Geophysicae*, 6, 31-38, 1988.